Transverse electron scattering response function of ^{3}He

Sara Della Monaca,[1] Victor D. Efros,[2] Avas Khugaev,[3] Winfried Leidemann,[1,4]
Giuseppina Orlandini,[1,4] Edward L. Tomusiak,[5] and Luping P. Yuan[1]
[1]*Dipartimento di Fisica, Università di Trento, I-38100 Trento, Italy*
[2]*Russian Research Centre "Kurchatov Institute", RU-123182 Moscow, Russia*
[3]*Institute of Nuclear Physics, Uzbekistan Academy of Sciences, Tashkent, Uzbekistan*
[4]*Istituto Nazionale di Fisica Nucleare, Gruppo Collegato di Trento, Italy*
[5]*Department of Physics and Astronomy, University of Victoria, Victoria, British Columbia V8P 1A1, Canada*
(Received 18 January 2008; published 28 April 2008)

The transverse response function $R_T(q,\omega)$ for ^{3}He is calculated using the configuration space BonnA nucleon-nucleon potential, the Tucson-Melbourne three-body force, and the Coulomb potential. Final states are completely taken into account via the Lorentz integral transform technique. Nonrelativistic one-body currents plus two-body π and ρ meson exchange currents (MECs) as well as the Siegert operator are included. The response R_T is calculated for $q = 174$, 250, 400, and 500 MeV/c and in the threshold region at $q = 174$, 324, and 487 MeV/c. Strong MEC effects are found in low- and high-energy tails, but due to MECs there are also moderate enhancements of the quasielastic peak (6–10%). The calculation is performed both directly and via transformation of electric multipoles to a form that involves the charge operator. The contribution of the latter operator is suppressed in and below the quasielastic peak, while at higher energies the charge operator represents almost the whole MEC contribution at the lowest q value. The effect of the Coulomb force in the final state interaction is investigated for the threshold region at $q = 174$ MeV/c. Its neglect enhances R_T by more than 10% in the range up to 2 MeV above threshold. In a comparison with experimental data, one finds relatively good agreement at $q = 250$ and 400 MeV/c, while at $q = 500$ MeV/c, presumably due to relativistic effects, the theoretical quasielastic peak position is shifted to somewhat higher energies. The strong MEC contributions in the threshold region are nicely confirmed by data at $q = 324$ and 487 MeV/c.

DOI: 10.1103/PhysRevC.77.044007 PACS number(s): 25.30.Fj, 21.45.−v, 21.30.−x

I. INTRODUCTION

Electromagnetic interactions in the trinucleon systems play an important role in testing NN and $3N$ forces as well as nucleonic current operators. Among the many reaction observables available are the response functions which determine the inclusive electron scattering cross section

$$\frac{d^2\sigma}{d\Omega\, d\omega} = \sigma_{\rm Mott}\left[\frac{Q^4}{q^4}R_L(q,\omega) + \left(\frac{Q^2}{2q^2} + \tan^2\frac{\theta}{2}\right) R_T(q,\omega)\right], \quad (1)$$

where ω is the electron energy loss, q is the magnitude of the electron momentum transfer, θ is the electron scattering angle, and $Q \equiv \{\mathbf{q},\omega\}$, $Q^2 = q^2 - \omega^2$. $R_L(q,\omega)$ and $R_T(q,\omega)$ are called the longitudinal and transverse response functions, respectively. To calculate either of these response functions, one needs to be able to take into account all final states (usually in the continuum) which are connected to the ground state via the current or charge operators. This can be accomplished in several ways. For example recent calculations of these response functions by Golak *et al.* [1] and Deltuva *et al.* [2] base their calculations on Faddeev techniques, whereas we employ the Lorentz integral transform (LIT) [3,4] method. A recent review article on the LIT approach is given in Ref. [5].

The longitudinal response is driven by the nuclear charge density operator and has recently been calculated covering large parts of the nonrelativistic regime in Refs. [1,2,4]. It is notable that although some of these groups use considerably different calculational techniques, they obtain similar results for $R_L(q,\omega)$. All these nonrelativistic calculations of $R_L(q,\omega)$ show quite good agreement with experiment for modest momentum transfers, i.e., $q < 400$ MeV/c. However for larger q the position of the quasielastic peak is sensitive to relativistic corrections in the kinetic energy. In Ref. [6] the nonrelativistic calculation was extended up to $q = 700$ MeV/c by choosing a proper reference frame, where relativistic effects on the kinetic energy are minimized. A subsequent transformation of the theoretical results to the laboratory frame led, in fact, to a much better agreement with data. Concerning the realistic NN interaction model, there appears to be a relative insensitivity to which model is used. As far as $3N$ forces are concerned, there is no unique picture. For ^{3}He their inclusion improves the agreement with data, whereas for ^{3}H one observes the opposite effect [4].

In $R_T(q,\omega)$ it is the nuclear transverse current density that drives the response. This current density can be expressed as the sum of various components: the normal one-body currents with their relativistic corrections, two-body currents arising from meson exchange NN forces (MECs) and isobar excitations, three-body currents arising from NNN forces. In Ref. [1], the AV18 NN potential [7] with the UrbanaIX NNN potential [8] were used and one-body currents as well as π and ρ MECs were taken into account to calculate $R_T(q,\omega)$ at $q = 200$, 300, 400, and 500 MeV/c and the low-energy R_T at various q. In Ref. [2], the CD-Bonn potential and its coupled-channel extension CD-Bonn+Δ [9] was taken. The one-body current, π and ρ MECs, and Δ currents were

considered. In addition to computing R_T at $q = 300$ and 500 MeV/c, near-threshold responses at various q were also shown.

Here we present the first fully realistic computation of R_T with the LIT method (in Ref. [10] the LIT method was applied to the R_T of ^{4}He but with approximations for the MEC and using a semirealistic NN potential only). Our present calculations are carried out in coordinate space, and therefore we have to use a configuration space NN potential. We take the BonnA potential [11] (hereinafter referred to as BonnRA) together with the Tucson-Melbourne (TM′) [12] NNN potential to calculate the response at $q = 174$, 250, 400, and 500 MeV/c and at $q = 324$ and 487 MeV/c in the near-threshold region. We would like to point out that the LIT method allows us to include consistently the Coulomb interaction in initial and final states, which is not done in Refs. [1,2]. For the electromagnetic current operator, we include the nonrelativistic one-body operators plus, as in Refs. [1,2], the π and ρ two-body MECs.

We chose the BonnRA potential because it is a boson exchange based potential. With such a potential, the form of the MEC is uniquely determined by explicit knowledge of the boson-nucleon coupling. For phenomenological NN potentials such as the AV18, which was used in Ref. [1], one can construct a consistent current $\mathbf{j}$ so that $i\nabla \cdot \mathbf{j}$ is equal to the commutator of the Hamiltonian with the nuclear charge operator (any purely transverse current piece can be added without having any impact on the gauge condition above) [13–16]. For consistent π and ρ MECs, one uses the following model. Potential terms with the same operator structure as appearing in π and ρ exchange potentials are parametrized in terms of a π- and ρ-like exchange. This then leads to a π- and ρ-like MEC which is consistent with such potential terms but is not equivalent to a genuine π/ρ MEC. For example, it could happen that a part of the ρ-like exchange is effectively parametrized in terms of ρ-like mesons with a lower mass than the physical ρ. We think that the use of such a consistent MEC is rather safe and should lead to quite realistic descriptions of MEC contributions. Nonetheless, here we prefer to work with the unique π and ρ MECs of the BonnRA potential, since MEC contributions based on such a potential model are probably even safer. Of course, the BonnRA potential is not one of the modern high-precision NN potentials; it has to be considered as a realistic NN model of some lower quality. On the other hand, one may ask if this fact is relevant to the R_T case considered here. In our previous paper on R_L [4], we made various comparisons between BonnRA plus TM′ $3N$-force and AV18 plus UIX $3N$-force results (in the same kinematic region as in present paper). Differences are quite small; in fact, they are much smaller than the present precision of experimental data. There is no reason that this should be different for R_T if one considers only one-body currents. And as to the corresponding MEC, the unique BonnRA current is certainly not worse than the AV18 π- and ρ-like MECs.

Our calculation is performed in two ways depending on how we treat the electric multipole operators. One method, which we refer to as the direct method, simply uses the current operators *per se* in the electric multipoles. In the second method, the electric multipole operators are transformed via the use of the continuity equation into a form which includes the charge operator. We refer to this latter form of the electric multipole operator as the Siegert form. If both the continuity equation were fulfilled exactly and dynamic equations were solved exactly, then these two ways would lead to the same results. Since, as in our case, a realistic nuclear force includes components additional to one-boson exchange potentials, such as momentum-dependent NN forces and $3N$ forces, the continuity equation is only approximately fulfilled when one employs only the dominant, well-established MECs. Therefore performing calculations in the two ways allows us, on the one hand, to find out to what extent the π and ρ exchange currents we use are compatible with the realistic nuclear force employed. On the other hand, via use of the charge operator, it permits us to take into account a part of the additonal MECs, thus checking their possible relevance. In Refs. [1,2] such an investigation was not carried out (in Ref. [1] the Siegert operator is only used for reactions with real photons).

II. NUCLEAR FORCES AND THE CURRENT OPERATOR

The transverse response R_T which depends on the transverse nuclear current density operator $\mathbf{J}_T$ is given by

$$R_T(q,\omega) = \overline{\sum}_{M_0} \int\!\!\!\!\!\!\int df \, \langle \Psi_0 | \mathbf{J}_T^\dagger(\mathbf{q},\omega) | \Psi_f \rangle \cdot \langle \Psi_f | \mathbf{J}_T(\mathbf{q},\omega) | \Psi_0 \rangle \, \delta[E_f - E_0 + q^2/(2M_T) - \omega]. \tag{2}$$

Here M_T is the mass of the target nucleus, Ψ_0 and Ψ_f denote the ground and final states, respectively, while E_0 and E_f are their eigenenergies,

$$(h - E_0)\Psi_0 = 0, \quad (h - E_f)\Psi_f = 0, \tag{3}$$

where h is the intrinsic nuclear nonrelativistic Hamiltonian. States of our system are represented by products of normalized center-of-mass plane waves $\varphi(\mathbf{P}_{0,f})$ and internal substates $\Psi_{0,f}$ entering Eq. (2). Correspondingly, the current operator $\mathbf{J}$ in Eq. (2) is related to the primary current operator $\bar{\mathbf{J}}$ as follows,

$$\mathbf{J}\,\delta(\mathbf{P}_f - \mathbf{P}_0 - \mathbf{q}) = \langle \varphi(\mathbf{P}_f) | \bar{\mathbf{J}} | \varphi(\mathbf{P}_0) \rangle, \tag{4}$$

where the matrix element is defined in the center-of-mass subspace. The cross section we need corresponds to the laboratory reference frame, and we set in Eq. (4) $\mathbf{P}_0 = 0$. The quantity $\mathbf{J}_T$ is that component of $\mathbf{J}$ which is orthogonal to $\mathbf{q}$. The second summation (integration) in Eq. (2) goes over all final states belonging to the same energy E_f, and M_0 is the projection of the ground state angular momentum J_0.

The Hamiltonian h includes the kinetic energy terms, the $2N$ and $3N$ force terms, and the proton Coulomb interaction term. As in Ref. [4], the ground state Ψ_0 is calculated via an expansion in basis functions which are correlated sums of products of hyperradial functions, hyperspherical harmonics, and spin-isospin functions. In the present work, the $2N + 3N$ interactions are taken as the Coulomb+BonnRA+TM′ ($\Lambda = 2.835$ fm^{-1}) as in Ref. [4]. The TM′ cutoff parameter Λ properly fixes the ^{3}H binding energy to 8.47 MeV.

We perform a nonrelativistic calculation. The current $\mathbf{J}$ includes one- and two-body operators. The one-body current operator as obtained from Eq. (4) is

$$\mathbf{j}^{(1)} = \sum_{k=1}^{A} [\mathbf{j}(k)_{\rm spin} + \mathbf{j}(k)_p + \mathbf{j}(k)_q],$$

where A is the number of nucleons in the target nucleus and

$$\mathbf{j}(k)_{\rm spin} = e^{i\mathbf{q}\cdot\mathbf{r}'_k} \frac{i(\sigma_k \times \mathbf{q})}{2M} G_M(k),$$
$$\mathbf{j}(k)_p = e^{i\mathbf{q}\cdot\mathbf{r}'_k} \frac{\mathbf{p}'_k}{M} G_E(k),$$
$$\mathbf{j}(k)_q = e^{i\mathbf{q}\cdot\mathbf{r}'_k} \frac{\mathbf{q}}{2M} G_E(k).$$

Here $\mathbf{r}'_k = \mathbf{r}_k - \mathbf{R}_{\rm c.m.}$, $\mathbf{p}'_k = \mathbf{p}_k - \mathbf{P}_{\rm c.m.}/A$, and σ_k are the relative coordinate, momentum, and spin operator of the kth particle and M denotes the nucleon mass, while $\mathbf{R}_{\rm c.m.}$ and $\mathbf{P}_{\rm c.m.}$ are the center-of-mass coordinate and momentum variables of the A-body system. The component $\mathbf{j}_q$ does not contribute to $\mathbf{J}_T$. However, separate multipoles as defined below depend on this component.

In the above expressions we use the notation

$$G_{E,M}(k) = G^p_{E,M}(Q^2)\frac{1+\tau_{zk}}{2} + G^n_{E,M}(Q^2)\frac{1-\tau_{zk}}{2}, \quad (5)$$

where $G^{p,n}_{E,M}$ are the Sachs form factors and τ_{zk} denotes the third component of the isospin operator of the kth nucleon. With our procedure the computational labor is reduced when the number of ω-dependent form factors is reduced [5]. To this end, we use the approximation

$$G^n_E(Q^2) \approx G^p_E(Q^2)\gamma\left(Q^2_{av}\right), \quad (6)$$

where $\gamma(Q^2_{av}) = G^n_E(Q^2_{av})/G^p_E(Q^2_{av})$, $Q^2_{av} = q^2 - \omega^2_{av}$ and $\omega_{av} = q^2/(2M)$. Similarly for the one-body spin current, we use

$$G^p_M(Q^2) \approx \bar{\mu}_p\left(Q^2_{av}\right)G^p_E(Q^2), \quad \bar{\mu}_p\left(Q^2_{av}\right) = \frac{G^p_M\left(Q^2_{av}\right)}{G^p_E\left(Q^2_{av}\right)}, \quad (7)$$

$$G^n_M(Q^2) \approx \bar{\mu}_n\left(Q^2_{av}\right)G^p_E(Q^2), \quad \bar{\mu}_n\left(Q^2_{av}\right) = \frac{G^p_M\left(Q^2_{av}\right)}{G^p_E\left(Q^2_{av}\right)}. \quad (8)$$

For the usual dipole magnetic form factors, as used in this work, the above relations are fulfilled exactly, and we have checked that the approximation provides a very good accuracy for G^n_E. In a future extension of our work to a high-q region, $q > 500$ MeV/c, we will use more sophisticated nucleon form factor fits. In these cases, the above relations are only approximately fulfilled, although we have checked that they still lead to excellent accuracy. The neutron electric form factor we use here is taken from Ref. [17] as used in Ref. [18]. With Eqs. (6)–(8), the one-body current is replaced by $\mathbf{j}^{(1)} \to G^p_E(Q^2)\mathbf{J}^{(1)}$ where $\mathbf{J}^{(1)}$ is now given by

$$\mathbf{J}^{(1)}(\mathbf{q}) = \sum_{k=1}^{A} \frac{e^{i\mathbf{q}\cdot\mathbf{r}'_k}}{M} \left\{ \left(\mathbf{p}'_k + \frac{\mathbf{q}}{2}\right)\left[\frac{1+\tau_{zk}}{2} + \gamma\left(Q^2_{av}\right)\frac{1-\tau_{zk}}{2}\right] + \frac{i(\sigma_k \times \mathbf{q})}{2}\left[\bar{\mu}_p\left(Q^2_{av}\right)\frac{1+\tau_{zk}}{2} + \bar{\mu}_n\left(Q^2_{av}\right)\frac{1-\tau_{zk}}{2}\right]\right\}. \quad (9)$$

The dominant contributions to the two-body current $\mathbf{J}^{(2)}$ arise from the π and ρ meson exchange currents. These currents are usually expressed in terms of "seagull" and "true exchange" pieces. Thus we write here

$$\mathbf{J}^{(2)} = \mathbf{j}^{\pi}_{\rm SG} + \mathbf{j}^{\pi}_{\rm ex} + \mathbf{j}^{\rho}_{\rm SG} + \mathbf{j}^{\rho}_{\rm ex}. \quad (10)$$

We list in Appendix A the coordinate space representations of these currents with the corresponding values of coupling constants, etc. Momentum space forms of these meson exchange currents are related to these coordinate space forms, apart from the multiplicative isovector electric form factor $G^v_E(Q^2) = (G^p_E(Q^2) - G^n_E(Q^2))/2$, via

$$\mathbf{j}^b_a(\mathbf{q})e^{i\mathbf{q}\cdot\mathbf{R}_{\rm c.m.}} = \int d^3x\, e^{i\mathbf{q}\cdot\mathbf{x}}\, \mathbf{j}^b_a(\mathbf{x}), \quad (11)$$

where the superscripts and subscripts correspond to those in the right-hand side of Eq. (10).

Finally we use the current operator $\mathbf{J}$ in the form

$$\mathbf{J} = G^p_E(Q^2)\mathbf{J}^{(1)} + 2G^v_E(Q^2)\mathbf{J}^{(2)}. \quad (12)$$

III. MULTIPOLE EXPANSION OF THE TRANSVERSE RESPONSE

The dynamic calculations are performed in separate subspaces belonging to fixed angular momentum J and its projection M (see also Ref. [5]). One can account for M dependencies analytically by performing a multipole expansion of R_T. To this end we use a decomposition into multipoles of the transverse current. This decomposition will also allow us to employ an alternative expression for the transition operator, see below. The transverse current is represented as

$$\mathbf{J}_T = 4\pi \sum_{\lambda={\rm el,mag}} \sum_{jm} i^{j-\epsilon}\, \mathcal{T}^{\lambda}_{jm}(q)\mathbf{Y}^{(\lambda)*}_{jm}(\hat{\mathbf{q}}). \quad (13)$$

Here $\hat{\mathbf{q}} = q^{-1}\mathbf{q}$ and $\mathbf{Y}^{(\lambda)}_{jm}$ are electric and magnetic vector spherical harmonics [19] and $\epsilon = 0$ when $\lambda = $ el, or $\epsilon = 1$ when $\lambda = $ mag. This then allows the transverse response to be written as

$$R_T(q,\omega) = \frac{4\pi}{2J_0+1} \sum_{\lambda={\rm el,mag}} \sum_{Jj} (2J+1)(R_T)^{j\lambda}_J, \quad (14)$$

where

$$(R_T)^{j\lambda}_J = \sum\!\!\!\!\!\!\int df \left\langle q^{j\lambda}_{JM}\middle|\Psi_f(J,M)\right\rangle\left\langle\Psi_f(J,M)\middle|q^{j\lambda}_{JM}\right\rangle \times \delta(E_f - E_0 - \omega), \quad (15)$$

J and M are the final state angular momentum and its projection, and $|q^{j\lambda}_{JM}\rangle$ is given by

$$\left|q^{j\lambda}_{JM}\right\rangle = \left[\mathcal{T}^{\lambda}_j \otimes \left|\Psi_0(J_0)\right\rangle\right]_{JM}. \quad (16)$$

In Eq. (15), M is arbitrary.

In terms of the more standard multipoles and vector spherical harmonics $\mathbf{Y}^l_{jm}$, we can write

$$\mathcal{T}^{\rm el}_{jm} = \left(\frac{j+1}{2j+1}\right)^{1/2} T^{j-1}_{jm} + \left(\frac{j}{2j+1}\right)^{1/2} T^{j+1}_{jm}, \quad (17)$$

$$\mathcal{T}^{\rm mag}_{jm} \equiv T^{j}_{jm} \quad (18)$$

where

$$T^l_{jm} = \frac{1}{4\pi i^{j-\epsilon}} \int d\Omega_{\mathbf{q}} \left(\mathbf{Y}^l_{jm}(\hat{\mathbf{q}}) \cdot \mathbf{J}(\mathbf{q},\omega)\right). \quad (19)$$

Since charge has to be conserved, it is well known that the above expression for $\mathcal{T}^l_{jm}$ can be rewritten as

$$\mathcal{T}^{\rm el}_{jm} = \left(\frac{j+1}{j}\right)^{1/2} \frac{\omega}{q}\rho_{jm} + \left(\frac{2j+1}{j}\right)^{1/2} T^{j+1}_{jm}, \quad (20)$$

where ρ_{jm} is a charge multipole of the charge density operator ρ defined by

$$\rho_{jm}(q) = \frac{1}{4\pi i^j} \int d\Omega_{\mathbf{q}} Y_{jm}(\hat{\mathbf{q}})\rho(\mathbf{q}). \quad (21)$$

We shall refer to the form of $\mathcal{T}^{\rm el}_{jm}$ in Eq. (17) as the direct form and to that in Eq. (20) as the Siegert form. The first term of Eq. (20) will be called the Siegert operator, while the second term is the residual term. Appendix B gives the multipole operators T^l_{jm} for the one-body currents, while Appendix C lists them for the π and ρ exchange currents.

IV. CALCULATION OF THE RESPONSE

The techniques we use in calculating the response have been largely set out in Ref. [4]. Here we add some extra detail which arises in the case of the transverse response. The Lorentz transform of the partial response $(R_T)^{j\lambda}_J$ of Eq. (15) is given by

$$\Phi^{j\lambda,\alpha}_J(q,\sigma_R,\sigma_I) = \sum_n \frac{(R_T)^{j\lambda,\alpha}_J(q,\omega_n)}{(\omega_n-\sigma_R)^2+\sigma_I^2} + \int d\omega \frac{(R_T)^{j\lambda,\alpha}_J(q,\omega)}{(\omega-\sigma_R)^2+\sigma_I^2}. \quad (22)$$

The sum in Eq. (22) corresponds to transitions to discrete levels with excitation energy ω_n. In our $A=3$ case, there exists only one discrete contribution corresponding to $M1$ elastic scattering. In Eq. (22) the response is supplied with an additional superscript α. It specifies separate contributions to the response $(R_T)^{j\lambda}_J$ of Eq. (15), e.g., a given α determines the isospin of the final state. In addition, it specifies contributions that correspond to components of the multipole operators with different nucleon form factor dependencies.

It was pointed out above that one- and two-body currents have different ω dependencies through their different form factors. Therefore we need to calculate the responses with the individual parts of the current, i.e., $\mathbf{J}^{(1)}\mathbf{J}^{(1)}$, $\mathbf{J}^{(1)}\mathbf{J}^{(2)}$, and $\mathbf{J}^{(2)}\mathbf{J}^{(2)}$. The corresponding partial response functions will carry the superscripts $\alpha = \{11, 12, 22\}$ so that the response $(R_T)^{j\lambda}_J$ would be expressed as

$$(R_T(q,\omega))^{j\lambda}_J = \left(G^p_E(Q^2)\right)^2 (R_T(q,\omega))^{j\lambda,11}_J + 4G^p_E(Q^2)G^v_E(Q^2)(R_T(q,\omega))^{j\lambda,12}_J + 4\left(G^v_E(Q^2)\right)^2 (R_T(q,\omega))^{j\lambda,22}_J. \quad (23)$$

Additional ω dependence of the electric multipole operators arises when they are used in the Siegert form, i.e., in the form of Eq. (20). Because of the additional ω dependence of the first term in Eq. (20), we calculate separately the response originating from this term ($\sim\omega^2$), the response originating from the second term in Eq. (20), and the cross-term response ($\sim\omega$). For the same reason as in Eq. (23), each of these responses is in turn broken into the one-body piece, the two-body piece, and the cross piece, which are calculated separately. The superscript α in Eq. (22) enumerates all these various cases, so that the response $(R_T)^{j,\rm el}_J$ is a sum of the responses $(R_T)^{j\lambda,\alpha}_J$ multiplied by products of nucleon form factors times ω^n, $n=0,1,2$.

As described in Ref. [3], the transforms are determined dynamically. In the present case the transforms $\Phi^{j\lambda,\alpha}_J$ are obtained from

$$\Phi^{j\lambda,\alpha}_J(q,\sigma_R,\sigma_I) = \langle \tilde{\psi}^{j\lambda,\alpha}_{JM} | \tilde{\psi}^{j\lambda,\alpha}_{JM} \rangle, \quad |\tilde{\psi}^{j\lambda,\alpha}_{JM}\rangle = [h-\sigma_R+i\sigma_I]^{-1}|q^{j\lambda,\alpha}_{JM}\rangle. \quad (24)$$

The calculation (24) is M independent and is performed in separate subspaces belonging to given isospin and parity. Parities are determined by the multipole order j and the choice of $\lambda =$ el/mag. For a given λ, parity, and J, only one value of j is possible in our case.

To pass to responses, one needs to invert the transforms. This may be done either separately for each transform $\Phi^{j\lambda,\alpha}_J$ using Eq. (22) or for their sums at the same α. One may define the responses $R^\alpha_T = \sum_{\lambda={\rm el,mag}} R^{\lambda,\alpha}_T$, where [cf. Eq. (14)]

$$R^{\lambda,\alpha}_T(q,\omega) = \frac{4\pi}{2J_0+1}\sum_{Jj}(2J+1)(R_T)^{j\lambda,\alpha}_J(q,\omega). \quad (25)$$

One also defines the corresponding transforms

$$\Phi^{\lambda,\alpha}(q,\sigma_R,\sigma_I) = \frac{4\pi}{2J_0+1}\sum_{Jj}(2J+1)\Phi^{j\lambda,\alpha}_J(q,\sigma_R,\sigma_I). \quad (26)$$

They are related to the responses in Eq. (25) in the same way as in Eq. (22). All the various $\Phi^{\lambda,\alpha}$ are inverted separately to get $R^{\lambda,\alpha}_T$. Our inversion method and more information concerning the inversion can be found in Refs. [5,20,21]. We take $\sigma_I = 20$ MeV and distinguish between the two isospin cases $T=1/2$ and $3/2$, since the corresponding responses have different thresholds and thus the inversion can be carried out more precisely. After having inverted both cases, we sum up the two results. For the magnetic part of the response, we invert the $M1$ transition to the final state with $J^\pi = \frac{1}{2}^+$ separately, since, as mentioned above, it contains an elastic contribution. This elastic contribution can easily be determined by choosing a very small value for σ_I, and thereafter its effect

on the transform can be subtracted leading to a LIT of a purely inelastic response.

As mentioned earlier, charge conservation leads to the equality of the Siegert and direct forms of the transverse electric multipole operator. This provides an important check on our procedures especially with respect to the implementation of the MECs. The BonnRA potential contains more than just π and ρ meson exchange, but we expect that taking account of MECs from only these two exchanged particles should lead to the dominant MEC contribution in our kinematic range, while additional MEC effects are partially taken care of by the Siegert operator. A good test for the implementation of the MEC is provided by using a simple $\pi + \rho$ OBEP (one boson exchange potential) with their corresponding MECs. In this case, charge conservation should be exact, and the transverse response should be independent of whether one uses the Siegert or the direct form of $T^{\rm el}_{jm}$. We have made such tests at $q = 10$, 300, and 500 MeV/c and found very good agreement between the results of the two calculations [22].

V. RESULTS AND DISCUSSION

We have selected the momentum transfers $q = 174, 250, 400$, and 500 MeV/c for a calculation of $R_T(q, \omega)$ in a large ω range. In addition, we have considered the low-ω part of R_T at $q = 174$, 324, and 487 MeV/c, for which cases we took a maximal value of $J = 7/2$. For the other q values, a different choice for $J^{\max}$ was made: 11/2 ($q = 250$ MeV/c), $15/2(q = 400)$, and $19/2(q = 500)$. We have checked that with these settings, very good convergence of the multipole expansions of R_T are obtained in the requested energy ranges.

In the discussion, we compare results calculated with the various current operators of Sec. II (both with direct and Siegert forms) representing the following contributions: (a) one-body, (b) one-body and implicit MEC via Siegert operator, (c) one-body, π and ρ MEC, and (d) one-body, π and ρ MEC plus additional MEC via Siegert operator. If the exact charge conservation is satisfied, then the results of the direct calculation (c) will agree with those of the Siegert form (d).

In Figs. 1 and 2, we show the various current contributions to R_T. It is readily seen that there are rather strong MEC effects: 15–30 MeV above threshold MECs enhance R_T by more than 30% for the two higher q values (very close to threshold even by up to 200%, see Fig. 4); they increase the quasielastic peak height by 10% ($q = 174, 250$ MeV/c), 7% ($q = 400$), and 6% ($q = 500$); for lower q they also lead to large effects in the high-energy tail [e.g., at pion threshold, increases of 180% ($q = 174$ MeV/c), 95% ($q = 250$), 22% ($q = 400$), and 5% ($q = 500$)]. In general, relative contributions of MECs are determined mainly by distances $|\omega - \omega_{\rm peak}|$. This is natural, since the peaks correspond to maximum contributions of one-body operators.

It is also seen that Siegert contributions remain quite small in and below the quasielastic peak. On the other hand, they become more important with increasing energy (e.g., at pion threshold and $q = 174$ (250) MeV/c, enhancements are of 130% (55%) of the one-body contribution). In addition to the fact that in general MEC contributions are rather small in the peak as compared to one-body contributions, Siegert contributions are strongly suppressed in and below the peak by the factor ω/q in Eq. (20). The approximate transition operator we discuss takes account of MEC only via the Siegert operator, i.e., the charge operator from Eq. (20). As seen in Fig. 2, in the tail region this approximation provides the response rather close to the true one at the lowest q value, $q = 174$ MeV/c. This agrees with the well-known fact that in moderate energy photodisintegration processes ($\omega = q$), MEC contributions are largely included by the Siegert operator.

It is interesting to note that there exist additional Siegert MEC contributions beyond the π and ρ MECs entering the direct calculation. This is because the π and ρ exchanges constitute only the dominating part of a consistent exchange current with the BonnRA potential. Other two-body currents are induced by momentum and spin-orbit dependent potential

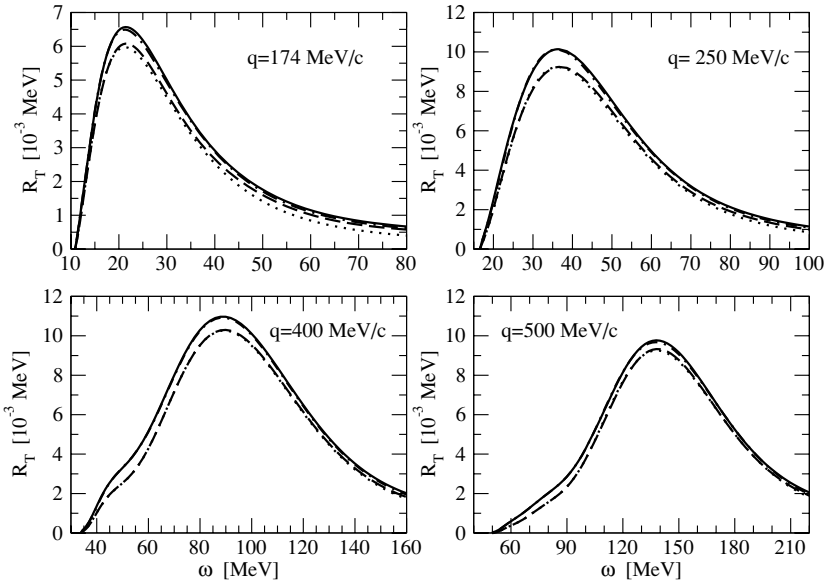

FIG. 1. Effects of the various contributions on R_T in the quasielastic region at $q = 174$, 250, 400, and 500 MeV/c: one-body (dotted), one-body + implicit MEC via Siegert operator (dashed), one-body + π and ρ MEC taken into account directly (dashed-dotted), one-body + implicit MEC via Siegert operator + additional π and ρ MEC contributions (solid).

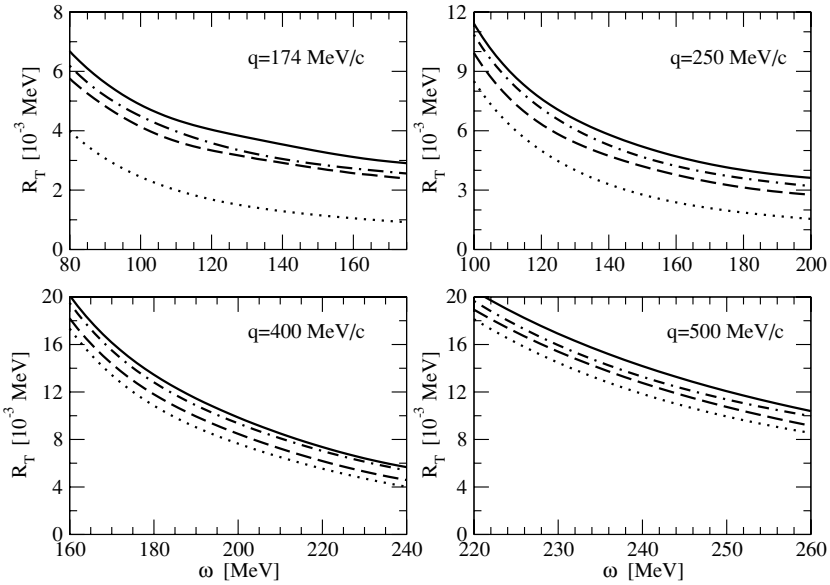

FIG. 2. Same as Fig. 1, but for the high-energy region.

terms. In addition, three-body currents, originating from the TM-3NF, could lead to Siegert contributions. Effects of the Siegert operator beyond the π and ρ MECs were also found in the proton-deuteron radiative capture with the BonnCD+Δ potential [23]. It is seen from Figs. 1 and 2 that such effects are small for energies far from the photon point. Indeed, there, the complete calculation via direct inclusion of MEC operators and the complete alternative calculation that involves the Siegert operator have led to results close to each other. However, closer to the photon point, the additional Siegert contributions can lead to corrections of the order of 10%.

In Fig. 3, we show our R_T results in comparison with experimental data. For $q = 250$ and 400 MeV/c, one finds good agreement. However, data are not precise enough to allow a definite conclusion about the MEC contribution. As opposed to the lower q cases, we find at $q = 500$ MeV/c a difference between the theoretical and experimental peak positions. The shift amounts to about 5–10 MeV. Relativistic effects, in particular those arising from corrections to the kinetic energy, might be responsible for this difference. In fact, in Ref. [6] it was shown for the longitudinal response function $R_L(q, \omega)$ that such effects lead at $q = 500$ MeV/c to a shift of the peak position by 6 MeV.

In Fig. 4, we depict various R_T theoretical and experimental low-energy results at $q = 0.882$, 1.64, and 2.47 fm^{-1} corresponding to about 174, 324, and 487 MeV/c, respectively. We do not show the contribution of the Siegert operator, since, as shown in Fig. 1, its effect is very small at low energies. One sees that the MEC contribution can be very important, e.g., at $q = 487$ MeV/c one finds an increase of about 200% close to threshold. Contrary to the cases shown in Fig. 3, here one can make a definite conclusion about the MEC contributions. It is evident that they lead to a considerably improved agreement between theory and experiment. For the two higher q values, theoretical and experimental results agree very well, whereas for $q = 174$ MeV/c the theoretical result underestimates experimental data somewhat below 10 MeV. A better theoretical description of the $q = 174$ MeV/c data is found in Ref. [1], where the AV18 NN potential and the UrbanaIX $3N$ force is used as the nuclear interaction. However, the Coulomb force was not included in the final

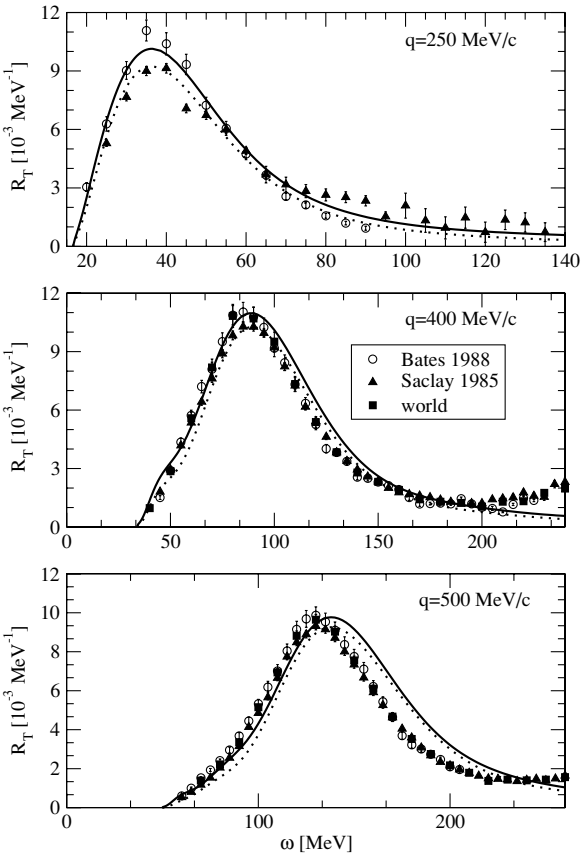

FIG. 3. Comparison of theoretical and experimental R_T at $q =$ 250, 400, and 500 MeV/c. Theoretical R_T with contributions: one-body (dotted) and one-body + π-MEC + ρ-MEC + additional MEC via Siegert operator (solid). Experimental data from Refs. [24] (triangles), [25] (circles), and [26] (squares).

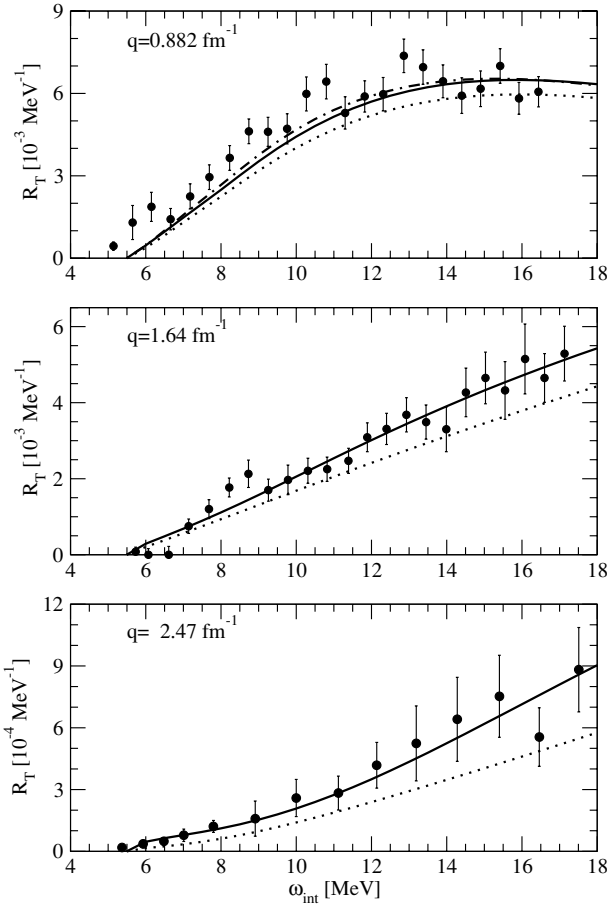

FIG. 4. Comparison of theoretical and experimental low-energy R_T at $q = 0.882$, 1.64, and 2.47 fm^{-1}. Notation of curves is the same as in Fig. 3, but an additional curve in the upper panel shows the total result when the Coulomb force is neglected in the final state interaction (dash-dotted). Experimental data are from Ref. [27].

state interaction. The effect of such neglect is illustrated in Fig. 4 for the case in discussion. Within 2 MeV above threshold it leads to an increase of more than 10%, while at 5 MeV above threshold the effect still amounts to 4%. In this way the theoretical results are shifted closer to the experimental data, but the effect is too small to reach a good agreement at low energies.

We summarize our results as follows. We have calculated the transverse form factor $R_T(q, \omega)$ considering besides one- and two-body currents also the so-called Siegert operator. As the nuclear interaction, we took the BonnRA NN potential and the Tucson-Melbourne TM′ $3N$ force. Since we are particularly interested in the MEC effects and the role of the Siegert operator, we chose the BonnRA potential, for which the important π and ρ exchange currents are directly determined by the potential model. It is true that also for more phenomenological NN potentials, e.g., AV18, consistent π and ρ MECs can be constructed [13–15], but to this end one has to interpret the isovector part of the phenomenological potential as an effective π and ρ exchange.

We find that MECs provide very strong contributions both at lower energies and in the high-energy tail while giving a moderate increase to the height of the quasielastic peak. Siegert contributions are unimportant in and below the quasielastic peak. They become considerably more sizable at higher energies, but additional MEC contributions have also to be taken into account; thus a calculation in which, in addition to the one-body current, MEC currents are taken into account via only the Siegert operator is not sufficient. On the other hand, a calculation with only one-body currents plus π and ρ MECs may also not be sufficient at higher energies, since, as we have shown, effects due to additional two- and three-body currents can become important. To include at least a part of these additional exchange effects, it is better to work also in this case with the operator in Siegert form. The appropriate place to study the structure of MECs is the energy region below the quasielastic peak. Indeed, the contributions of MECs are large in this region, whereas they are rather small in the peak, and beyond the peak they are partly represented by the Siegert operator, i.e., the charge operator.

Relatively good agreement with experimental data is obtained at $q = 250$ and 400 MeV/c, while at $q = 500$ MeV/c, presumably because of relativistic effects, the position of the theoretical quasielastic peak is located somewhat above the experimental one. Close to threshold, one finds very strong MEC contributions. They are necessary in order to achieve a good description of the experimental data at $q = 324$ and 487 MeV/c. Also at $q = 174$ MeV/c, they lead to an improved agreement with experiment; but in the range from threshold to 5 MeV above, the theoretical result underestimates the data somewhat.

In the future, we plan to investigate the momentum range 500 MeV/$c \leqslant q \leqslant 1$ GeV/c considering relativistic corrections for the one-body current operator and performing the calculation in a reference frame where relativistic effects in the kinetic energy are minimized [6]. We also plan to study isobar current contributions including $\Delta(1232)$ degrees of freedom.

ACKNOWLEDGMENTS

Financial support from the Russian Foundation for Basic Research, Grant 07-02-01222-a (V.D.E.) and the National Science and Engineering Research Council of Canada (E.L.T.) is acknowledged.

APPENDIX A: CONFIGURATION SPACE π AND ρ MECS

For convenience, we list below the well-known π and ρ configuration space exchange currents.

$$\mathbf{j}^{\pi}_{\mathrm{SG}}(\mathbf{x}) = \frac{f_0^2}{m_\pi^2} \sum_{i<j} (\tau_i \times \tau_j)_z \times [(\sigma_i \cdot \nabla_i)\sigma_j \delta(\mathbf{x} - \mathbf{r}_j) - (\sigma_j \cdot \nabla_j)\sigma_i \delta(\mathbf{x} - \mathbf{r}_i)] \times \sum_{k=1}^{3} h_k^{\pi} Y\left(\mu_k^{\pi}, |\mathbf{r}_i - \mathbf{r}_j|\right), \quad \text{(A1)}$$

$$\mathbf{j}^{\pi}_{\rm ex}(\mathbf{x}) = \frac{1}{4\pi}\frac{f_0^2}{m_\pi^2}\sum_{i<j}(\tau_i\times\tau_j)_z(\sigma_i\cdot\nabla_i)(\sigma_j\cdot\nabla_j) \times\sum_{k=1}^{3}h_k^{\pi}\big[Y\big(\mu_k^{\pi},|\mathbf{x}-\mathbf{r}_j|\big)\nabla_{\mathbf{x}}Y\big(\mu_k^{\pi},|\mathbf{x}-\mathbf{r}_i|\big) - Y\big(\mu_k^{\pi},|\mathbf{x}-\mathbf{r}_i|\big)\nabla_{\mathbf{x}}Y\big(\mu_k^{\pi},|\mathbf{x}-\mathbf{r}_j|\big)\big], \quad (A2)$$

$$\mathbf{j}^{\rho}_{\rm SG}(\mathbf{x}) = \frac{1}{4\pi}\left(\frac{g_\rho}{2M}\right)^2\left(1+\frac{f_\rho}{g_\rho}\right)^2\sum_{i<j}(\tau_i\times\tau_j)_z \times\big[(\sigma_i\times\nabla_i)\times\sigma_j\delta(\mathbf{x}-\mathbf{r}_j) - (\sigma_j\times\nabla_j) \times\sigma_i\delta(\mathbf{x}-\mathbf{r}_i)\big]\sum_{k=1}^{3}h_k^{\rho}Y\big(\mu_k^{\rho},|\mathbf{r}_i-\mathbf{r}_j)|\big). \quad (A3)$$

$$\mathbf{j}^{\rho}_{\rm ex}(\mathbf{x}) = \frac{1}{(4\pi)^2}\left(\frac{g_\rho}{2M}\right)^2\left(1+\frac{f_\rho}{g_\rho}\right)^2 \times\sum_{i<j}(\tau_i\times\tau_j)_z\,(\sigma_i\times\nabla_i)\cdot(\sigma_j\times\nabla_j) \times\sum_{k=1}^{3}h_k^{\rho}\big[Y\big(\mu_k^{\rho},|\mathbf{x}-\mathbf{r}_j|\big)\nabla_{\mathbf{x}}Y\big(\mu_k^{\rho},|\mathbf{x}-\mathbf{r}_i|\big) - Y\big(\mu_k^{\rho},|\mathbf{x}-\mathbf{r}_i|\big)\nabla_{\mathbf{x}}Y\big(\mu_k^{\rho},|\mathbf{x}-\mathbf{r}_j|\big)\big]. \quad (A4)$$

Here $Y(m,r)=e^{-mr}/r$. We list the coupling constants, the masses μ_k^α, and the regularization constants h_k^α, where $\alpha=\pi$ or ρ, taken from Ref. [11]:

$$f_0^2=\frac{1}{4\pi}f_{\pi NN}^2=0.0805,\quad \frac{g_\rho^2}{4\pi}=1.2,\quad \frac{f_\rho}{g_\rho}=6.1, \quad (A5)$$

$$\mu_1^\alpha=m_\alpha,\quad \mu_2^\alpha=\Lambda_\alpha+10\ \text{MeV},\quad \mu_3^\alpha=\Lambda_\alpha-10\ \text{MeV}, \quad \Lambda_\pi=1.3\ \text{GeV},\quad \Lambda_\rho=1.2\ \text{GeV}, \quad (A6)$$

$$h_1^\alpha=1,\quad h_2^\alpha=-\frac{\big(\mu_3^\alpha\big)^2-\big(\mu_1^\alpha\big)^2}{\big(\mu_3^\alpha\big)^2-\big(\mu_2^\alpha\big)^2},\quad h_3^\alpha=\frac{\big(\mu_2^\alpha\big)^2-\big(\mu_1^\alpha\big)^2}{\big(\mu_3^\alpha\big)^2-\big(\mu_2^\alpha\big)^2}. \quad (A7)$$

APPENDIX B: T^l_{jm} MULTIPOLES OF ONE-BODY CURRENTS

In the following, the nonrelativistic expressions of the electric and magnetic multipoles for the one-body currents are written. Each of them is decomposed in a convection and a spin current. For the magnetic multipoles one has

$$T^j_{jm}=\sum_i\big[T^{j,\,\rm spin}_{jm}(i)+T^{j,\,\rm conv}_{jm}(i)\big], \quad (B1)$$

with

$$T^{j,\rm spin}_{jm}(i)=\frac{1}{M}\frac{q}{2}\left(\frac{\overline{\mu}_p+\overline{\mu}_n}{2}+\frac{\overline{\mu}_p-\overline{\mu}_n}{2}\tau_{zi}\right) \times\left\{\sqrt{\frac{j}{2j+1}}\,j_{j+1}(qr_i')[Y_{j+1}(\hat{\mathbf{r}}_i')\otimes\sigma_i]_{jm} -\sqrt{\frac{j+1}{2j+1}}\,j_{j-1}(qr_i')[Y_{j-1}(\hat{\mathbf{r}}_i')\otimes\sigma_i]_{jm}\right\}, \quad (B2)$$

$$T^{j,\rm conv}_{jm}(i)=\frac{1}{M}\left(\frac{1+\gamma}{2}+\frac{1-\gamma}{2}\tau_{zi}\right) \times j_j(qr_i')[Y_j(\hat{\mathbf{r}}_i')\otimes\partial_i']_{jm}. \quad (B3)$$

The quantity ∂'_μ is defined by the relationship $-i\partial'_\mu=p'_\mu$. If the last Jacobi vector is defined as $\vec{\xi}_{A-1}=\sqrt{(A-1)/A}\,[\mathbf{r}_A-(A-1)^{-1}\sum_{i=1}^{A-1}\mathbf{r}_i]$, then

$$\partial_\mu'^{(A)}=\left[\frac{A-1}{A}\right]^{1/2}\frac{\partial}{\partial\xi_{A-1,\mu}}.$$

Similarly, we write the one-body multipoles contributing to $\mathcal{T}^{\rm el}_{jm}$ as

$$T^l_{jm}=\sum_i\big[T^{l,\rm spin}_{jm}(i)+T^{l,\rm conv}_{jm}(i)\big], \quad (B4)$$

where $l=j\pm1$. One obtains

$$T^{j\pm1,\,\rm spin}_{jm}(i)=-\frac{1}{M}\frac{q}{2}\left(\frac{\overline{\mu}_p+\overline{\mu}_n}{2}+\frac{\overline{\mu}_p-\overline{\mu}_n}{2}\tau_{zi}\right) \times\sqrt{\frac{j+(1\mp1)/2}{2j+1}}\,j_j(qr_i')[Y_j(\hat{\mathbf{r}}_i')\otimes\sigma_i]_{jm} \quad (B5)$$

and

$$T^{j\pm1,\rm conv}_{jm}(i)=\pm\frac{1}{M}\left(\frac{1+\gamma}{2}+\frac{1-\gamma}{2}\tau_{zi}\right) \times\left\{j_{j\pm1}(qr_i')[Y_{j\pm1}(\hat{\mathbf{r}}_i')\otimes\partial_i']_{jm} -\frac{q}{2}\sqrt{\frac{j+(1\pm1)/2}{2j+1}}\,j_j(qr_i')Y_{jm}(\hat{\mathbf{r}}_i')\right\}. \quad (B6)$$

The term proportional to $j_j(qr_i')$ in Eq. (B6) above cancels when one forms the electric multipole from Eq. (17).

APPENDIX C: T^L_{JM} MULTIPOLES OF π AND ρ MECS

Here the T^L_{JM} multipoles are given for the "12" pair. The total result should be multiplied by 3 to account for three pairs of identical particles in the trinucleons.

(i) π seagull

$$T^L_{JM}=\frac{\sqrt{4\pi}}{i^{J-\epsilon}}\left(\frac{f_0}{m_\pi}\right)^2\sum_{\ell\rho\sigma}\sum_{\sigma'\mathcal{L}}i^{\sigma'-\ell}(-1)^{\sigma+\mathcal{L}+J} \times[1+(-1)^{\ell+\rho}]\hat{\ell}^2\hat{\rho}\hat{L}\hat{\sigma}\hat{\sigma}'\hat{\mathcal{L}}\begin{pmatrix}\ell&1&\sigma\\0&0&0\end{pmatrix} \times\begin{pmatrix}\sigma'&\ell&L\\0&0&0\end{pmatrix}\begin{Bmatrix}L&\ell&\sigma'\\\sigma&\mathcal{L}&1\end{Bmatrix}\begin{Bmatrix}L&1&\mathcal{L}\\\rho&J&1\end{Bmatrix} \times j_{\sigma'}(qz)j_\ell\left(\frac{qr}{2}\right)(H^\pi(r))'\big[[Y_{\sigma'}(\hat{\mathbf{z}})\otimes Y_\sigma(\hat{\mathbf{r}})]^{\mathcal{L}} \otimes\Sigma^{[\rho]}_{12}\big]^J_M(\tau_1\times\tau_2)_z. \quad (C1)$$

Here $\mathbf{r} = \mathbf{r}_2 - \mathbf{r}_1$, $\mathbf{z} = -[(\mathbf{r}_1 + \mathbf{r}_2)/2 - \mathbf{R}_{\rm c.m.}]$, $\hat{\mathbf{r}} = \mathbf{r}/r$, $\hat{\mathbf{z}} = \mathbf{z}/z$, $\left(H^\pi(r)\right)' = dH^\pi(r)/dr$, and $H^\pi(r) = \sum_{k=1}^3 h_k^\pi\, Y(\mu_k^\pi, r)$, where the constants are given by Eqs. (A5) and (A7). We denote the spin-coupling $[\sigma_1 \otimes \sigma_2]_{\rho,m}$ by $\Sigma_{12}^{\rho,m}$.

(ii) π exchange current. The multipole for the true π exchange is the sum

$$T^L_{JM} = T^{L,X1}_{JM} + T^{L,X2}_{JM} + T^{L,X3}_{JM},$$

where

$$\begin{aligned} T^{L,X1}_{JM} = &-\frac{\sqrt{4\pi}}{i^{J-\epsilon}}\frac{4}{\pi}\left(\frac{f_0}{m_\pi}\right)^2 \\ &\times \sum_{\ell\rho\sigma\sigma'}\sum_{L'\mathcal{L}} i^{\sigma+\sigma'+1}(-1)^\sigma(\hat{\ell})^2\hat{\rho}\hat{L}(\hat{L}')^2\hat{\sigma}\hat{\sigma}'\hat{\mathcal{L}} \\ &\times \begin{pmatrix} 1 & 1 & \rho \\ 0 & 0 & 0 \end{pmatrix}\begin{pmatrix} \sigma' & \ell & L \\ 0 & 0 & 0 \end{pmatrix}\begin{pmatrix} 1 & \ell & L' \\ 0 & 0 & 0 \end{pmatrix} \\ &\times \begin{pmatrix} L' & \rho & \sigma \\ 0 & 0 & 0 \end{pmatrix}\begin{Bmatrix} L' & \rho & \sigma \\ \mathcal{L} & \sigma' & J \end{Bmatrix}\begin{Bmatrix} 1 & \ell & L' \\ \sigma' & J & L \end{Bmatrix} \\ &\times j_{\sigma'}(qz)\Phi^{(3)}_{\sigma,\ell}(q,r)\big[[Y_{\sigma'}(\hat{\mathbf{z}}) \\ &\otimes Y_\sigma(\hat{\mathbf{r}})]^{\mathcal{L}} \otimes \Sigma_{12}^{[\rho]}\big]^J_M(\tau_1 \times \tau_2)_z, \end{aligned} \tag{C2}$$

$$\begin{aligned} T^{L,X_2}_{JM} = &\frac{\sqrt{4\pi}}{i^{J-\epsilon}}\frac{q^2}{\pi}\left(\frac{f_0}{m_\pi}\right)^2 \\ &\times \sum_{\ell\rho\sigma\sigma'}\sum_{L'\mathcal{L}} i^{\sigma+\sigma'+1}(-1)^{\sigma'}(\hat{\ell})^2\hat{\rho}\hat{L}(\hat{L}')^2\hat{\sigma}\hat{\sigma}'\hat{\mathcal{L}} \\ &\times \begin{pmatrix} 1 & 1 & \rho \\ 0 & 0 & 0 \end{pmatrix}\begin{pmatrix} \sigma' & \ell & L' \\ 0 & 0 & 0 \end{pmatrix}\begin{pmatrix} 1 & \ell & \sigma \\ 0 & 0 & 0 \end{pmatrix} \\ &\times \begin{pmatrix} L' & \rho & L \\ 0 & 0 & 0 \end{pmatrix}\begin{Bmatrix} L & \rho & L' \\ \mathcal{L} & 1 & J \end{Bmatrix}\begin{Bmatrix} 1 & \ell & \sigma \\ \sigma' & \mathcal{L} & L' \end{Bmatrix} \\ &\times j_{\sigma'}(qz)\Phi^{(1)}_{\sigma,\ell}(q,r)\big[[Y_{\sigma'}(\hat{\mathbf{z}}) \\ &\otimes Y_\sigma(\hat{\mathbf{r}})]^{\mathcal{L}} \otimes \Sigma_{12}^{[\rho]}\big]^J_M(\tau_1 \times \tau_2)_z, \end{aligned} \tag{C3}$$

$$\begin{aligned} T^{L,X_3}_{JM} = &-\frac{\sqrt{4\pi}}{i^{J-\epsilon}}\frac{4\sqrt{3}q}{\pi}\left(\frac{f_0}{m_\pi}\right)^2\sum_{\ell f\sigma\sigma'}\sum_{L'J'\mathcal{L}} \\ &\times i^{\sigma+\sigma'+1}(-1)^{\mathcal{L}+1}(\hat{\ell})^2\hat{L}(\hat{L}')^2\hat{\sigma}\hat{\sigma}'\hat{\mathcal{L}}(\hat{J}')^2(\hat{f})^2 \\ &\times \begin{pmatrix} 1 & \ell & J' \\ 0 & 0 & 0 \end{pmatrix}\begin{pmatrix} 1 & J' & \sigma \\ 0 & 0 & 0 \end{pmatrix}\begin{pmatrix} L & 1 & L' \\ 0 & 0 & 0 \end{pmatrix} \\ &\times \begin{pmatrix} L' & \ell & \sigma' \\ 0 & 0 & 0 \end{pmatrix}\begin{Bmatrix} L' & \ell & \sigma' \\ \sigma & \mathcal{L} & f \end{Bmatrix}\begin{Bmatrix} 1 & \ell & J' \\ \sigma & 1 & f \end{Bmatrix} \\ &\times \begin{Bmatrix} L' & f & \mathcal{L} \\ 1 & 1 & 1 \\ L & 1 & J \end{Bmatrix} j_{\sigma'}(qz)\Phi^{(2)}_{\sigma,\ell}(q,r)\big[[Y_{\sigma'}(\hat{\mathbf{z}}) \\ &\otimes Y_\sigma(\hat{\mathbf{r}})]^{\mathcal{L}} \otimes \Sigma_{12}^{[1]}\big]^J_M(\tau_1 \times \tau_2)_z. \end{aligned} \tag{C4}$$

Here $\Phi^{(n)}_{\sigma,\ell}(q,r) = \sum_{k=1}^3 h_k^\pi\, \phi^{(n)}_{\sigma,\ell}(q,r,\mu_k^\pi)$, where the functions $\phi^{(n)}_{\sigma,\ell}(q,r,m)$ are defined in Ref. [28]. The multipoles (C1)–(C4) are real.

(iii) ρ exchange currents. The multipoles of the ρ exchange currents can be obtained from the above π exchange currents by means of the following replacements: $\mu_k^\pi \to \mu_k^\rho$, $h_k^\pi \to h_k^\rho$,

$$\left(\frac{f_0}{m_\pi}\right)^2 \to \frac{1}{4\pi}\left(\frac{g_\rho}{2M}\right)^2\left(1 + \frac{f_\rho}{g_\rho}\right)^2, \tag{C5}$$

and by inserting into each equation above the factor

$$-6(-1)^\rho\begin{Bmatrix} 1 & 1 & 1 \\ 1 & \rho & 1 \end{Bmatrix}. \tag{C6}$$

[1] J. Golak, R. Skibinski, H. Witala, W. Glöckle, A. Nogga, and H. Kamada, Phys. Rep. **415**, 89 (2005).
[2] A. Deltuva, L. P. Yuan, J. Adam, and P. U. Sauer, Phys. Rev. C **70**, 034004 (2004).
[3] V. D. Efros, W. Leidemann, and G. Orlandini, Phys. Lett. **B338**, 130 (1994).
[4] V. D. Efros, W. Leidemann, G. Orlandini, and E. L. Tomusiak, Phys. Rev. C **69**, 044001 (2004).
[5] V. D. Efros, W. Leidemann, G. Orlandini, and N. Barnea, J. Phys. G **34**, R459 (2007).
[6] V. D. Efros, W. Leidemann, G. Orlandini, and E. L. Tomusiak, Phys. Rev. C **72**, 011002(R) (2005).
[7] R. B. Wiringa, V. G. J. Stoks, and R. Schiavilla, Phys. Rev. C **51**, 38 (1995).
[8] B. S. Pudliner, V. R. Pandharipande, J. Carlson, S. C. Pieper, and R. B. Wiringa, Phys. Rev. C **56**, 1720 (1997).
[9] R. Machleidt, Phys. Rev. C **63**, 024001 (2001).
[10] S. Bacca, H. Arenhövel, N. Barnea, W. Leidemann, and G. Orlandini, Phys. Rev. C **76**, 014003 (2007).
[11] R. Machleidt, Adv. Nucl. Phys. **19**, 189 (1989).
[12] S. A. Coon, M. D. Scadron, P. C. McNamee, B. R. Barrett, D. W. E. Blatt, and B. H. J. McKellar, Nucl. Phys. **A317**, 242 (1979); S. A. Coon and W. Glöckle, Phys. Rev. C **23**, 1790 (1981); S. A. Coon (private communication), giving the most recent parameters as $a' = -1.35\mu^{-1}$, $b = -2.86\mu^{-3}$, and $d = -0.64\mu^{-3}$.
[13] D. O. Riska, Phys. Scr. **31**, 471 (1985).
[14] A. Buchmann, W. Leidemann, and H. Arenhövel, Nucl. Phys. **A443**, 726 (1985).
[15] H. Arenhövel and M. Schwamb, Eur. Phys. J. A **12**, 207 (2001).
[16] L. E. Marcucci, M. Viviani, R. Schiavilla, A. Kievsky, and S. Rosati, Phys. Rev. C **72**, 014001 (2005).
[17] S. A. Platchkov, Nucl. Phys. **A510**, 740 (1990).
[18] P. E. Bosted, Phys. Rev. C **51**, 409 (1995).
[19] D. A. Varshalovich, A. N. Moskalev, and V. K. Khersonskii, *Quantum Theory of Angular Momentum* (World Scientific, Singapore, 1988).
[20] V. D. Efros, W. Leidemann, and G. Orlandini, Few-Body Syst. **26**, 251 (1999).
[21] D. Andreasi, W. Leidemann, Ch. Reiss, and M. Schwamb, Eur. Phys. J. A **24**, 361 (2005).
[22] S. della Monaca, Ph. D. thesis, University of Trento (2007).

[23] A. Deltuva, L. P. Yuan, J. Adam, A. C. Fonseca, and P. U. Sauer, Phys. Rev. C **69**, 034004 (2004).
[24] C. Marchand *et al*., Phys. Lett. **B153**, 29 (1985); J. Morgenstern (private communication).
[25] K. Dow *et al*., Phys. Rev. Lett. **61**, 1706 (1988); K. Dow (private communication).
[26] J. Carlson, J. Jourdan, R. Schiavilla, and I. Sick, Phys. Rev. C **65**, 024002 (2002); J. Jourdan (private communication).
[27] G. A. Retzlaff *et al*., Phys. Rev. C **49**, 1263 (1994).
[28] W. Fabian and H. Arenhövel, Nucl. Phys. **A258**, 461 (1976).